Space Sci Rev (2010) 150: 285–302
DOI 10.1007/s11214-009-9607-5

The Lunar Reconnaissance Orbiter Miniature Radio Frequency (Mini-RF) Technology Demonstration

Stewart Nozette · Paul Spudis · Ben Bussey · Robert Jensen · Keith Raney · Helene Winters · Christopher L. Lichtenberg · William Marinelli · Jason Crusan · Michele Gates · Mark Robinson

Received: 17 November 2008 / Accepted: 6 November 2009 / Published online: 13 January 2010

Abstract The Miniature Radio Frequency (Mini-RF) system is manifested on the Lunar Reconnaissance Orbiter (LRO) as a technology demonstration and an extended mission science instrument. Mini-RF represents a significant step forward in spaceborne RF technology and architecture. It combines synthetic aperture radar (SAR) at two wavelengths (S-band and X-band) and two resolutions (150 m and 30 m) with interferometric and communications functionality in one lightweight (16 kg) package. Previous radar observations (Earth-based, and one bistatic data set from Clementine) of the permanently shadowed regions of the lunar poles seem to indicate areas of high circular polarization ratio (CPR) consistent with volume scattering from volatile deposits (e.g. water ice) buried at shallow (0.1–1 m) depth, but only at unfavorable viewing geometries, and with inconclusive results. The LRO Mini-RF utilizes new wideband hybrid polarization architecture to measure the Stokes parameters of the reflected signal. These data will help to differentiate "true" volumetric ice reflections from "false" returns due to angular surface regolith. Additional lunar science investigations (e.g. pyroclastic deposit characterization) will also be attempted during the LRO extended mission. LRO's lunar operations will be contemporaneous with India's Chandrayaan-1, which carries the Forerunner Mini-SAR (S-band wavelength and 150-m resolution), and bistatic radar (S-Band) measurements may be possible. On orbit calibration, procedures for LRO

S. Nozette · P. Spudis
Lunar and Planetary Institute, 3600 Bay Area Blvd, Houston, TX 77058, USA

B. Bussey (✉) · R. Jensen · K. Raney · H. Winters
Applied Physics Laboratory, Laurel, MD 20723, USA
e-mail: Ben.Bussey@jhuapl.edu

C.L. Lichtenberg
Naval Air Warfare Center, China Lake, CA 93555, USA

W. Marinelli · J. Crusan · M. Gates
National Aeronautics and Space Administration, Washington, DC 20546, USA

M. Robinson
Arizona State University, Tempe, AZ, USA

Mini-RF have been validated using Chandrayaan 1 and ground-based facilities (Arecibo and Greenbank Radio Observatories).

Keywords Lunar Reconnaissance Orbiter · Mini RF · Lunar poles

1 Introduction

The Lunar Reconnaissance Orbiter (LRO) Mini-RF technology demonstration is the product of over a decade of development. Its objectives are: (1) Flight verification of an advanced lightweight RF technology for future NASA and DoD communications applications; (2) Demonstration of a hybrid-polarity Synthetic Aperture Radar (SAR) architecture; (3) Obtaining measurements of the lunar surface as a function of radar band (S and X) and resolution (150 m, 30 m) which could identify water ice deposits in the permanently shadowed polar regions; (4) Production of topographic data using interferometry (S-band) and SAR stereo techniques; and (5) Mapping of areas of interest identified by the Chandrayaan-1 Forerunner Mini-SAR experiment and other lunar instruments. Because Mini-RF provides its own illumination and can penetrate the near subsurface at meter scales, it will acquire data not obtained by any other LRO payload.

Over the previous decade, the Department of Defense (DoD) and commercial industry made significant strides in developing advanced lightweight RF technology for wireless communication, Unmanned Airborne Vehicles (UAVs), and tactical missiles. The Mini-RF hardware is based on DoD communications technology and methodology. Precursor Mini-RF technology was flight-tested by the Naval Research Laboratory (NRL) in the low Earth orbit on the USAF MightySat-2 and XSS-10 missions as a Space Ground Link System (SGLS). Other technologies developed for commercial wireless systems, UAVs, manned aircraft such as the F-18, and tactical missiles were also incorporated into the payload.

In 2004, the DoD and NASA initiated the Mini-RF program to develop and flight-test advanced lightweight radar and communication systems and NASA elected to apply the technology to lunar exploration by building two payloads. The first, "Forerunner" Miniature SAR (Mini-SAR), was developed and integrated into the Indian Space Research Organization (ISRO) Chandrayaan-1 as a NASA guest payload and the second, on the LRO spacecraft as a technology demonstration. Chandrayaan-1 was launched on October 22, 2008 and is conducting a two-year systematic lunar mapping investigation. The Forerunner Mini-SAR is currently mapping the lunar poles at S band with a resolution of 150 m and is providing heritage and experience to the LRO Mini-RF system. The Forerunner Mini-SAR had to operate in the lunar thermal and radiation environment, yet was simpler in design and operation, providing significant experience and reduction of risk for the more advanced LRO Mini-RF system (Spudis et al. 2009). The LRO Mini-RF affords NASA and the DoD an opportunity to flight-qualify lightweight technology for a range of applications, including deep space communications. The flexibility, reconfigurability, and capability of Mini-RF will be demonstrated by a communications and radar mode utilizing the same hardware. The constraints of a lunar mission (range, limited duty cycle over the poles) and the low mass of advanced lightweight RF technology allows a technology demonstration which met the payload constraints of both the Chandrayaan and LRO spacecraft, and provided an opportunity to collect unique and valuable lunar science data. The new technologies being qualified on LRO Mini-RF include: Microwave Power Module (MPM) based multi-frequency transmitter, wideband dual-frequency panel antenna, all digital receiver and waveform synthesizer incorporating

Table 1 Mini-RF technology comparison

Radar System Comparisons with Mini RF Technology						
	Radar Mass	DC Power Input	RF Power (average)	Band	Spacecraft Dry Mass	Orbit Altitude
DoD TACSAT (notional)	40 kg	1000 W	200 W	X	350 kg	500 km
Magellan	154 kg	1000 W	325 W	S	1035 kg	249 × 8543 km
SEASAT			1000 W	L	2300 kg	800 km
SIR-C	11,000 kg	3000–9000 W		L, C, X		Shuttle
Chandrayaan Mini-SAR	8.1 kg	<100 W	15 W	S	525 kg (includes 12 Instruments)	100 km
LRO Mini-RF	∼13 kg	∼150 W	25 W	S, X	∼1000 kg (includes 6 Instruments, 1 Tech Demo)	50 km

Communications System Comparison with Mini RF Technology							
System	Mass	DC Power Input	RF Power	Band	Data Rate	Spacecraft Dry Mass	Orbit Altitude
Standard DoD SGLS	5 kg (electronics)	30 W	5 W	L, S	1–2 Mbs	Various	LEO
NRL Mini RF SGLS	1.5 kg (electronics)	30 W	5 W	L, S	1–2 Mbs	∼100 kg	LEO
Clementine	4.0 kg (xponder) (14 kg system total w 2nd xponder)	30 W	5 W	S	128 kbs (Lunar)	224 kg	Lunar 5000 × 400 km
Commercial GEO/TTC	17 kg total (dual redundant)	40 W	8 W (single)	Ku	8 kbs (GEO)	2,600 kg	GEO
NASA Discovery	21 kg	170 W	50 W (average)	S, Ka	100 Mbs (Lunar)	1000 kg	Super GEO
Mini-RF Optimized for Communications	∼14 kg (includes Antenna)	∼175 W	50 W	S, Ka	100 Mbs	450 kg	Lunar

field programmable gate array (FPGA) and analog-to-digital conversion at 1 GHz sampling. The Mini-RF parts qualification program, which included commercial technology, allowed innovative components to gain space qualification. A comparison of the Mini-RF radar and communications performance with existing and previously flown technology, illustrating mass and performance improvements, is shown in Table 1.

1.1 Background of Investigation

The LRO Mini-RF payload will address key science questions during the LRO primary and extended missions. These include exploring the permanently shadowed polar regions

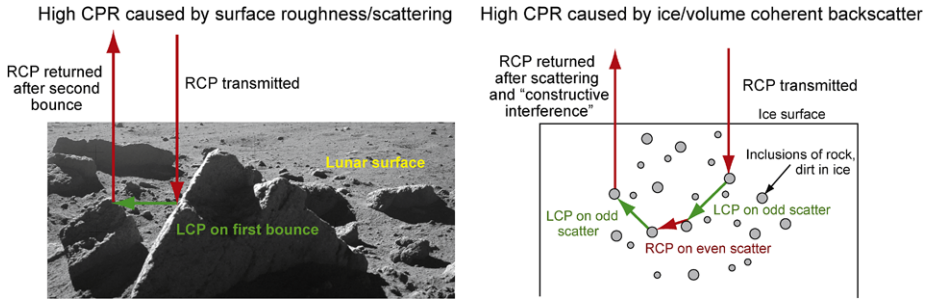

Fig. 1 Dual scattering caused by ice or roughness (from Spudis 2006)

and probing the lunar regolith in other areas of scientific interest (e.g. pyroclastic deposits). The nature and distribution of the permanently shadowed polar terrain of the Moon (e.g., Arnold 1979) has been the subject of considerable controversy. Initially, Arecibo monostatic radar measured the circular polarization ratio (CPR) in the region of the lunar South Pole; these data were interpreted to indicate the possible presence of ice on the lower wall of Shackleton crater (Stacy 1993). The presence of ice in the regolith causes a distinct, but not unique, CPR signature caused by the low-loss properties of ice and the Coherent Backscatter Opposition Effect (CBOE) (Fig. 1). Frozen volatiles have much lower transmission loss than silicate rocks, producing a higher average radar reflectivity. Total internal reflection also preserves the transmitted circular polarization sense in the scattered signal, which is also enhanced by constructive interference. The CBOE requires scattering centers (cracks or inhomogeneities) imbedded in a low-loss matrix such as ice (Mishchenko 1992). High CPR has been observed by radar in shadowed polar craters of Mercury. These results are generally attributed to total internal reflection and/or CBOE produced by low-loss frozen volatiles (e.g. ice) although other mechanisms have been proposed (Butler 1997). Data collected by the Clementine bistatic radar experiment (Nozette et al. 1996, 1997, 2001) also measured anomalous CPR in Shackleton as a function of bistatic angle, suggesting the presence of patchy, "dirty," ice deposits on the lower Earth facing wall. The high CPR region observed deepest within Shackleton crater also has a local angle of incidence of 50°, estimated by Stacy (1993). This wall has a monostatic CPR of 1.19 ± 0.12 (Stacy 1993) comparable to the radar bright feature at the North Pole of Mercury measured by Harmon and Slade (1992) that has generally been attributed to an ice deposit. Stacy (1993) noted that because this area may be permanently shadowed, the coherent backscatter opposition effect (CBOE) from ice deposits could be responsible for the enhanced CPR signature.

Subsequently, higher resolution Arecibo data were reported to be inconsistent with the previous measurements (Campbell et al. 2006), and it was suggested that all anomalous high CPR areas observed by Arecibo, near the lunar South Pole, were caused by rough surfaces as only some portions of these areas were believed to be permanently shadowed. It was also postulated (Simpson and Tyler 1999) that the Clementine polarization anomaly is only due to roughness and/or random noise in the data and not by the presence of ice. Campbell et al. (2006) suggested that the high CPR area within Shackleton crater could be due to diffuse backscatter from wavelength scale structures since other non-shadowed structures exhibit similar behavior.

Craters with diameters similar to Shackleton in regions that are fully illuminated (e.g., Shumberger G; Campbell et al. 2006) also show enhanced CPR signatures. The upper parts of the radar-facing inner rims of illuminated craters typically show greater backscatter cross

sections, most likely due to increased blockiness. However, the high CPR in Shackleton is deeper (further down the wall), isolated, discontinuous, and not associated with other geological units (roughness or layering), but its true depth is not observable from the Earth (Spudis 2006). Additionally, a high degree of correlation exists between the decreasing epithermal neutron flux and the shadowed terrain at the lunar South Pole, including Shackleton, which has been attributed to water ice deposits (Feldman et al. 1998, 2000; Elphic et al. 2007). New results from the Kaguya mission, which include low light imaging of the floor and lower walls of Shackleton, show these areas to be smooth and block free (Noda et al. 2008).

1.2 Mini-RF Measurement Objectives

The lunar ice controversy cannot be resolved with existing data. New measurements are required. Previous studies of mechanisms of deposition and preservation of lunar polar ice suggest that it may be buried at a depth of 0.1–2 m (Feldman et al. 2000). There is no precedent for a spaceborne imaging radar instrument that could probe the regolith at this depth for ice and meet the stringent mass and power constraints of the LRO spacecraft.

The Mini-RF architecture is new. The hybrid-polarity design (transmitting circular polarization, and receiving coherently two orthogonal linear polarizations) provides data sufficient to measure the 2×2 covariance matrix of the backscattered field, which in turn lead to the four Stokes parameters (Raney 2007). Analysis of these data, either by standard radar astronomy methods or by applying matrix decomposition techniques, extracts all information available in the radar reflections, thus providing a sharper tool than CPR alone to help differentiate between "true" (ice) and "false" (regolith blockiness) lunar returns.

2 Mini-RF Investigation Description

Mini-RF can operate as a dual-frequency, hybrid-polarity imaging radar designed to collect information about the scattering properties of the permanently dark areas near the lunar poles at optimum viewing geometry. As the LRO Mini-RF system probes the lunar regolith at two frequencies (S-band and X-band) it will provide additional information on the physical properties of the upper meter or two of lunar surface. Under the proposed observational constraints, Mini-RF can identify areas of high CPR ($\sim$1), which could be caused by ice deposits. Areas that do show high CPR can be analyzed with greater sensitivity through their backscattering features. It is hypothesized that "ice" and "regolith" will have differentiable characteristics as seen through their respective Stokes parameters at two wavelengths. When supported by Chandrayaan-1 and other LRO data (e.g. neutron spectroscopy, shadow and lighting, roughness and surface texture, thermal environment), the LRO Mini-RF measurements should provide more conclusive evidence as to the likelihood that ice deposits occur in permanently shadowed areas. Specific Mini-RF instrument requirements, performance, and data collection modes are shown in Table 2.

2.1 Technology Demonstrations

The Mini-RF observations are made possible within the mass and power constraints imposed by LRO via application of a number of technologies. Two key technologies are a wideband Microwave Power Module (MPM) based transmitter and a lightweight broadband antenna and polarization design. The LRO Mini-RF also has an S-band-only interferometric

Table 2 Mini-RF requirements and performance

	Requirements	Performance
Frequency	S and X Band	2380 Mhz (±10 Mhz) and 7140 Mhz (±10 MHz)
Mass	≤ 16 kg	13.9 kg total 8.5 kg electronics 5.4 kg antenna
Radiation Tolerance	20 KRad, SEU/SEL 75 MeV	Selective Wavers
Thermal Requirement	−20°C–30°C	
DC Current	< 4.8 A Transmitter < 4.7 A Remainder	5.2 A Transmitter 1.7 A at 27 V
		±0.25 dBm
		±0.3 dBm
RF Transmitter Power		42.6 dBm S Band 41.1 dBm X Band
Operating Time (Duty Cycle)	3 min on, 50 min off, 3 min on	10 min on, 20 min off, 10 min on (limit of test)
Transmit Polarization	Circular Polarization	Circular Polarization
Polarization Isolation	1.7 dB axial ratio	≤ 2.0 dB axial ratio (to be verified in flight)
Receive Polarization	H and V	≥ 40 dB Isolation
Channel to Channel Power	±1 dB "knowledge",	±0.2 dB S Band,
Calibration	−0.1 dB X band	±0.2 dB X Band
S Band Baseline Resolution	150 m azimuth × range	150 m×150 m
S Band Noise Equivalent	−30 dB at 50 km altitude	−33.6 dB
Radar Cross Section		
Number of Looks	16	16
Range Swath	6 km S band, 4 km X band	6 km S band, 4 km X band
S Band Zoom Capability	15 m × 30 m	15 m × 30 m
X Band Baseline Resolution	150 m	150 m × 150 m
X Band Noise Equivalent	−24 dB at 50 km altitude	−26.3 dB
Radar Cross Section		
Number of Looks	16	16
Pulse Rep Frequency	−18 dB	−18 dB
(2300–5000)/Ambiguity		
X Band Zoom Capability	30 m	15 × 30 m
Radiometric Stability	±0.5 dB	±0.5 dB
Communications Demonstration	S Band	2380 Mhz
Mode	Half Duplex	Half Duplex
Transmit	Modulated Signal	BPSK, Manchester Variable Data Rate and Modulation Index
Received Signal	Digitize Signal	Continuous 500 kbs

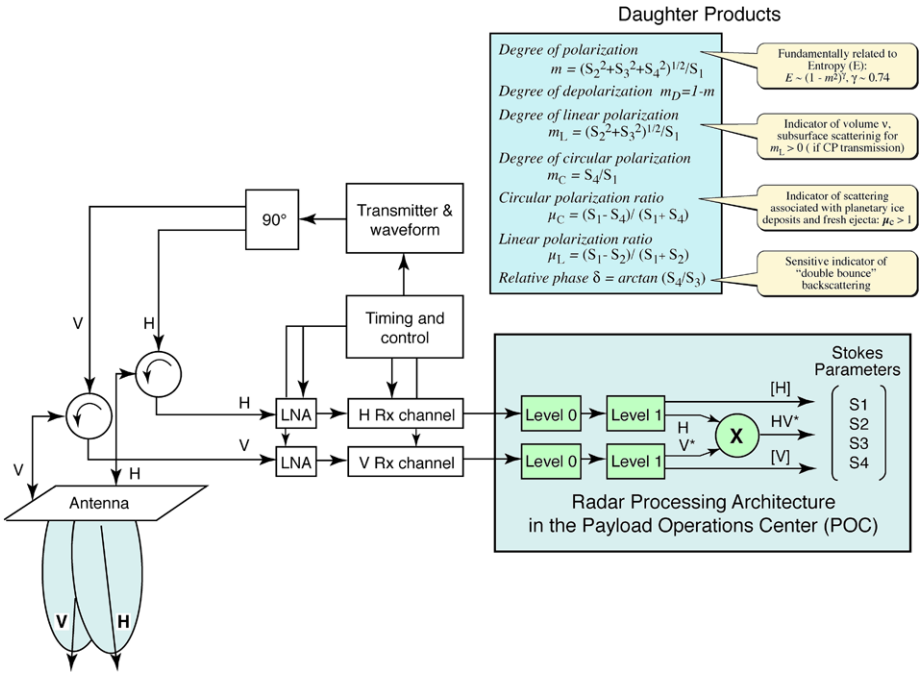

Fig. 2 Hybrid-polarity architecture

mode with 3.5-km wide strips with ±15-m mapping accuracy to measure lunar topography. This will be the first demonstration of interferometric SAR techniques in a planetary mission. The Mini-RF antenna architecture is shown in Fig. 2. This architecture is unique in planetary radar; it transmits right circular polarization radiation and receives the horizontal (H) and vertical (V) polarization components coherently, which are then reconstructed as Stokes' parameters during the data processing step. Both the communications and the radar astronomical objectives impose a requirement for circular polarization on the transmitted field. Conventional radar that would measure CPR then would have to be dual-circularly-polarized on receiver. The hybrid-polarity approach provides weight savings by eliminating circulator elements in the receiver paths, which reduces mass, increases RF efficiency, and minimizes cross-talk and other self-noise aspects of the received data. The H and V signals are passed directly to the ground-based processor. It is well known that the Stokes parameters comprise a full characterization of the backscattered field. The values of the four Stokes parameters do not depend on the choice of receiver polarization, so this architecture minimizes hardware while maintaining full science value. The result provides significant advantages over the conventional "CPR-measuring" dual-circular-polarized approach, yet the radar is simpler. The use of possible Stokes parameter-based products (e.g. CPR, degree-of-depolarization, degree-of-linear-polarization, phase "double bounce") have a number of significant advantages over traditional radar systems: less hardware is needed, resulting in fewer losses and a "cleaner," simpler flight instrument. The signal levels are comparable (within ∼2 dB) in both channels allowing relatively relaxed specifications on channel-to-channel cross-talk and more robust phase and amplitude calibration. The processor has a direct view through the entire receiver chain; including the antenna receives patterns and other radar parameters (e.g., gain and phase). These parameters are applied in processing

"Levels" (Level 0, 1) which correspond to successive data processing stages, as shown in Fig. 2. The design allows selective Doppler weighting to maximize channel–channel coherence (e.g., reduce the H & V beam mismatch). As CPR is less sensitive to channel imbalance by at least a factor of 2 with respect to explicit RCP/LCP, Stokes parameter-based backscatter decomposition strategies can help distinguish "false" from "true" high CPR areas (e.g., analysis of "m-δ" feature space; Raney 2007).

2.2 Concept of Operations

The Mini-RF concept of operations is shown in Fig. 3. Mini-RF has been allocated limited observation time so as not to interfere with collection of mapping data from other spacecraft instruments, particularly LROC imager, which like Mini-RF produces large amounts of data. During the normal mapping phase of LRO, Mini-RF is allocated two 10-minute collects to conduct communications demonstrations. Additionally, Mini-RF is allocated a 4-minute SAR collect and a 4-minute interferometry collect every month of the nominal mission. The designations "L" and "R" refer to the radar looking either "left" or "right" of the LRO orbital track. It may be possible to collect additional observations when the LROC imaging illumination is unfavorable. An imaging "season" refers to this period. The current plan is to identify high-value geological targets from the Forerunner Mini-SAR (Chandrayaan-1) systematic mapping and observe these areas using both the dual frequency of the LRO Mini-RF and the high-resolution zoom mode for specific areas. These data collects should allow better characterizations areas of high CPR, their geological settings, and the likelihood of a water ice composition.

By the end of the nominal LRO mission, Mini-RF will have collected regional S-band SAR maps from Forerunner Mini-SAR on Chandrayaan-1, 20 targeted SAR strips from Mini-RF on LRO, and correlation with higher resolution neutron and other data from LRO. Mini-RF could use observation opportunities from an extended LRO mission to acquire more data of both polar and non-polar regions. These data collection opportunities are currently defined as supplemental measurement goals, including additional SAR and interferometry data, additional communications experiment data, and bistatic options with the

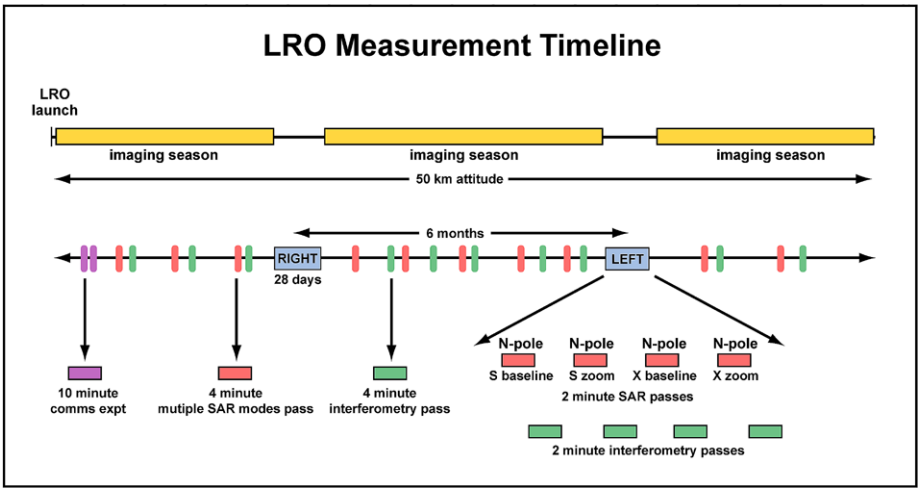

Fig. 3 An illustrative example of a possible LRO measurement sequence

Chandrayaan-1 instrument. High resolution "zoom" SAR imaging is also planned in support of the LCROSS experiment. Because both Chandrayaan-1 and LRO will be in lunar orbit at the same time, the Chandrayaan-1 and LRO Mini-RF units were designed to operate in a bistatic mode, with either Chandrayaan-1 or LRO transmitting and receiving in S-band. Both orbits cross at the poles and it may be possible to obtain bistatic measurements of selected polar targets to determine if high CPR is correlated with the bistatic (phase) angle. These observations, if possible, would be the most definitive in separating the effects of surface roughness from those of ice owing to the directional response of CBOE scattering from ice. The bistatic opportunities will require maneuvers to place both spacecraft near the same altitude so as to minimize the bistatic angle ($\leq 5°$).

3 Communication Technology Demonstration

The demonstration of Mini-RF in communications mode is a major objective of the LRO technology. By exercising the Mini-RF technology in this manner it may be space-qualified for future communications applications. While the data rates achieved are modest (85 kbs), these could be improved in future systems optimized for communications as shown in Table 1. Existing systems while capable of much higher data rates are heavier and not capable of multiple frequency multimode operation within the mass budget of Mini-RF (Table 1). Some of the communications objectives can be achieved with ground-based tests, but end-to-end far-field measurements under space radiation and thermal conditions, and space qualification of high voltage MPM technology, require flight testing. The Mini-RF frequency allocation (2380 MHz transmit and receive) is specified so as not to create interference with the LRO S-band communications system and is an approved planetary radar band. This frequency selection is compatible with Arecibo Observatory, which allows LRO to the Earth communications demonstrations. The LRO Mini-RF system will demonstrate half-duplex communication operation with ground assets during two 10-minute opportunities on Days 19–37 with additional times available during Days 38–57 of the mission. The demonstration opportunities are separated by minimum of 24 hours, followed by a 5-minute downlink demonstration, followed by a 5-minute uplink demonstration/calibration. In S-band (2380 MHz) uplink mode, the ground transmits a phase-modulated S-band signal; Mini-RF digitizes and records the raw data. The telemetered data is post-processed to achieve carrier lock and demodulation from Arecibo 2380 MHz transmissions by using a predefined waveform at 5 minutes per demonstration. In the downlink mode the Mini-RF phase modulates the transmitted signal while ground receivers perform carrier lock, bit sync, and data detection. The bit error rate is evaluated as a function of Eb/No to establish overall communication system performance. In the communications mode, Mini-RF provides 5–10 W peak RF power from its transmitter. The duty cycle is a function of input voltage and power consumption.

The transmit demonstration is limited to approximately 5-minute duration due to spacecraft average power requirements. S-Band direct modulation, including modulation direct on carrier, of BPSK at 85 kbs on the radar's transmit frequency will allow measurements of the Bit Error Rate (BER) performance. The link can support 220 kbps to the APL ground station. Mini-RF can gather statistically significant data and operate the payload within the allocated 5 minutes. Additional opportunities enabled by using antenna side lobes in view of the APL ground station will also be identified. These tests will modulate at a much lower rate to close the link using the side-lobe antenna pattern while the spacecraft is nominally pointed toward the APL ground station.

During the communication experiments, Mini-RF digitizes and records raw data with 100% duty cycle with a range decimation factor of 16, compatible with an LRO Space Wire data rate <30 Mbps. The limit to uplink power is due to large-aperture antenna (Arecibo) not overdriving the receiver. A compatibility test is not required and the communications test will be performed with commercial test equipment. In addition, a demonstration modulation using pseudo-random sequence at S-Band with the APL Ground System is planned with a BPSK modulation at 85 kbps modulation directly on carrier based on a Generator Polynomial within the radar with a sequence length of 32,767 bits. This strategy allows many repetitions of the sequence during the demonstration. The polynomials and modulation formats are compatible with CORTEX-XL ground receiver used at the APL ground station and with most conventional bit-error rate equipment. Compatibility testing with the APL ground station has been conducted.

4 Mini-RF Instrument Description

The Mini-RF Instrument is comprised of the following elements: (1) antenna, (2) transmitter, (3) digital receiver/quadrature detector waveform synthesizer, (4) analog RF receiver, (5) Control Processor, (6) interconnection module, and (7) supporting harness, RF cabling, and structures. The LRO Mini-RF system functional block diagram is shown in Fig. 4. The Mini-RF layout is shown in Fig. 5 and its installation on the LRO spacecraft is shown in Fig. 6.

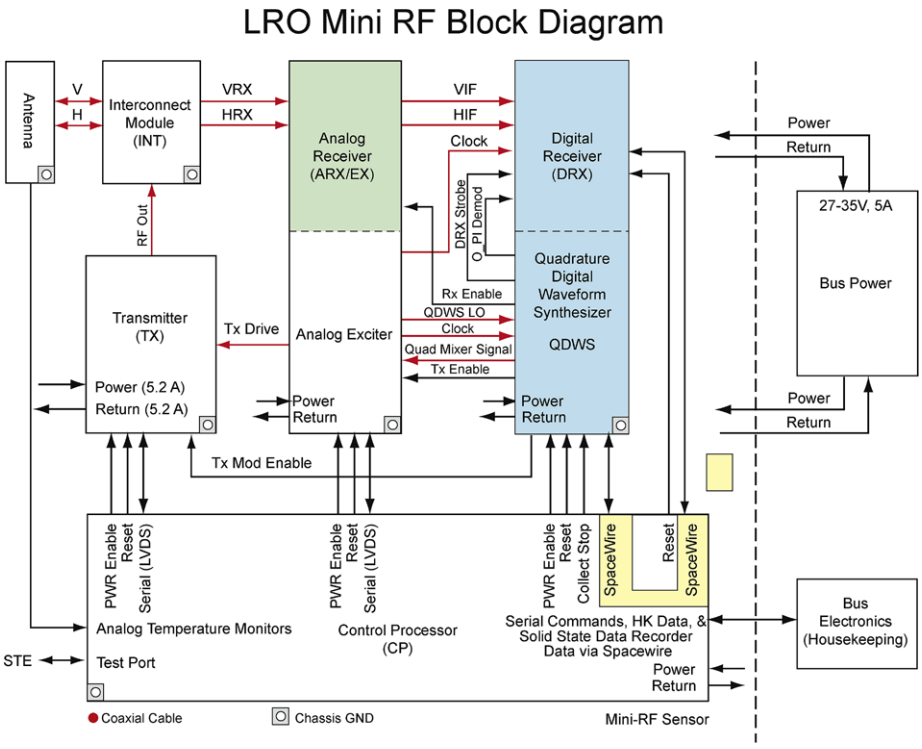

Fig. 4 LRO Mini-RF block diagram

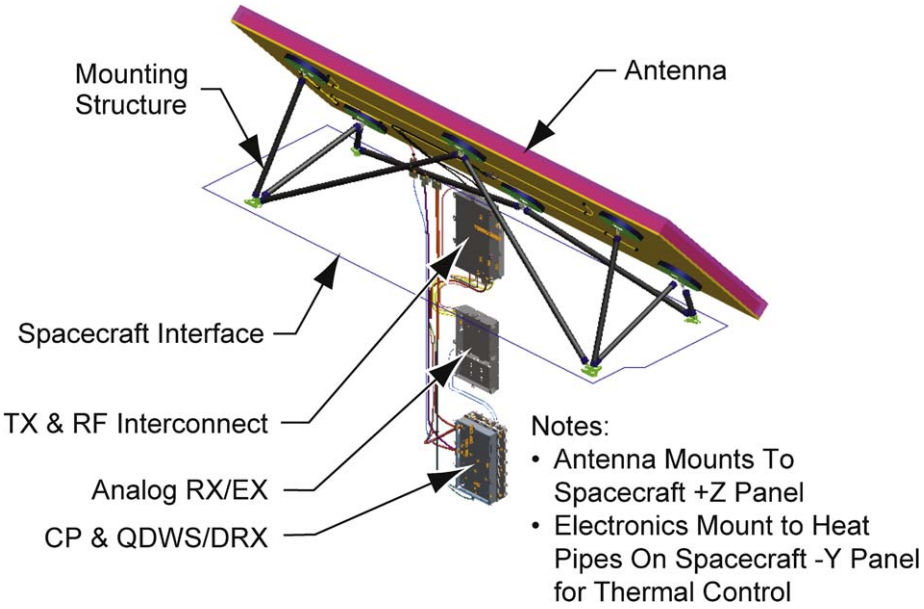

Fig. 5 LRO Mini-RF mechanical configuration

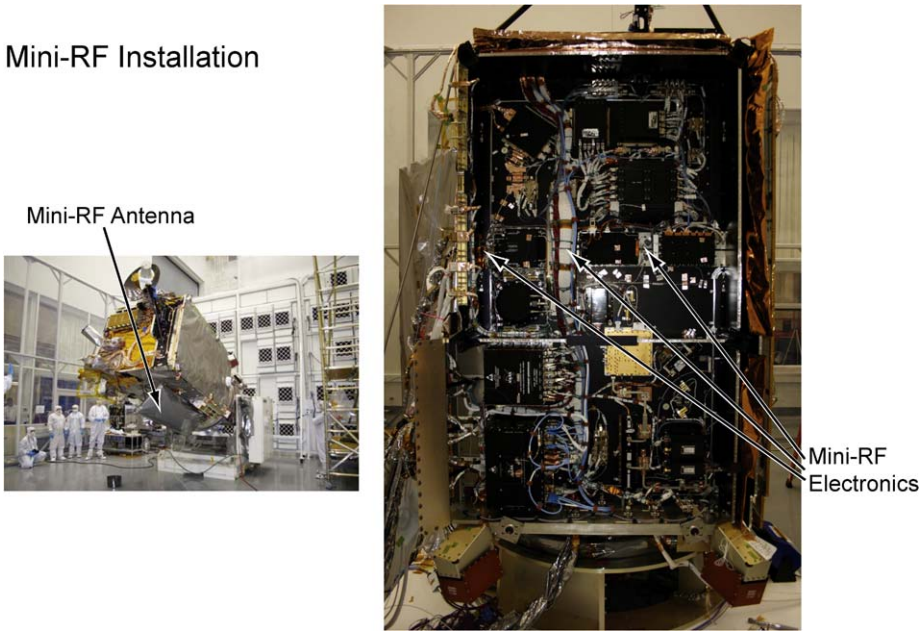

Fig. 6 Mini-RF on LRO spacecraft

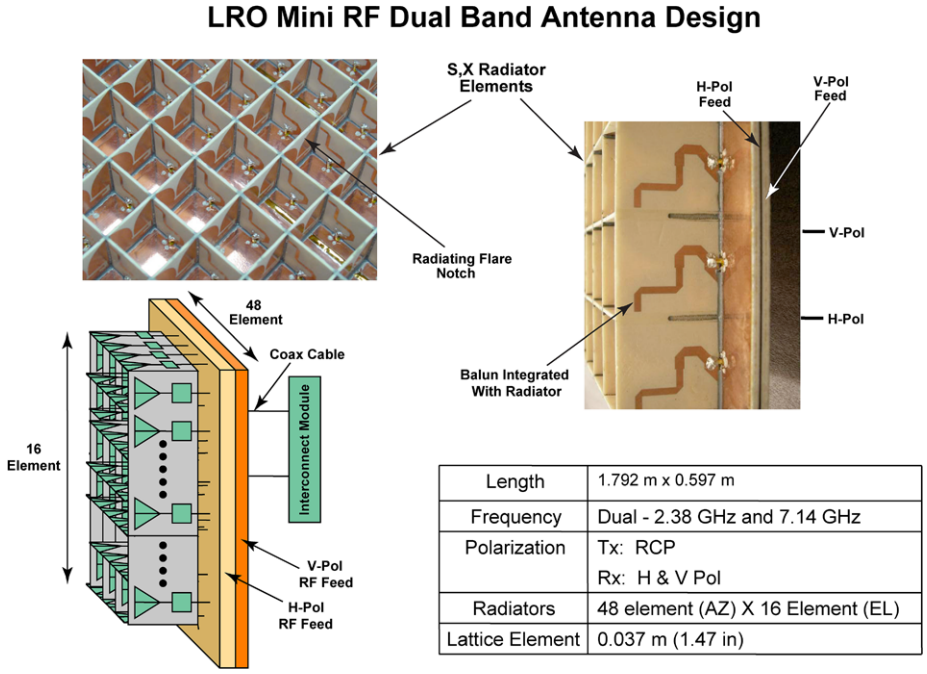

Fig. 7 Mini-RF antenna design

4.1 Antenna

An "egg crate" antenna (Fig. 7) allows a broadband, dual-frequency design with a single antenna panel, without any deployable mechanisms (e.g. feeds) while also meeting stringent weight and volume constraints. The elements are sized to allow a 3:1 frequency range. Each element incorporates radiators and physical phasing combines their power. The thermal design, materials selection, manufacturing, and test qualification heritage of single-frequency Chandrayaan Mini-SAR antenna was applied to the dual frequency LRO Mini-RF unit. Because of this heritage, the Mini-RF antenna is robust and lightweight (4 kg) while satisfying all technical requirements.

4.2 Transmitter

The LRO Mini-RF transmitter (Figs. 8, 9) takes full advantage of the capabilities of the wideband antenna. The transmitter is the first implementation of Microwave Power Module (MPM) technology on a long-duration spaceflight, which affords a significant breakthrough in available bandwidth and power efficiency with reduced mass as compared to previous traveling wave tube (TWT) systems (Fig. 10). The MPM combines a solid state RF driver/preamplifier with a traveling wave tube amplifier, a hybrid approach combining the advantages of both solid state and vacuum electronic technology. Flight-testing the MPM technology is a major goal of the Mini-RF demonstration. The MPM is enabling in giving Mini-RF its dual band capability within the challenging mass, power, and volume constraints of the LRO spacecraft. MPM technology has extensive heritage in airborne and other tactical systems but the Mini-RF development program had to make significant efforts to qualify

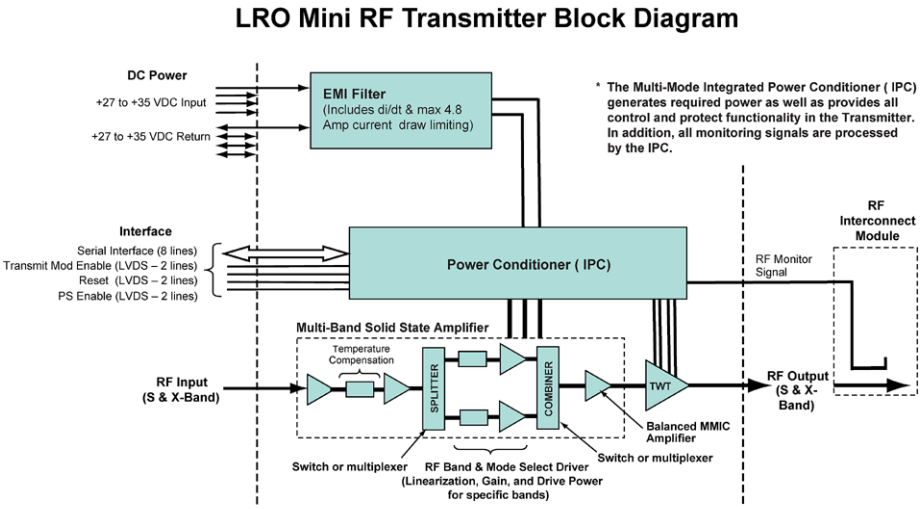

Fig. 8 Mini-RF transmitter block diagram

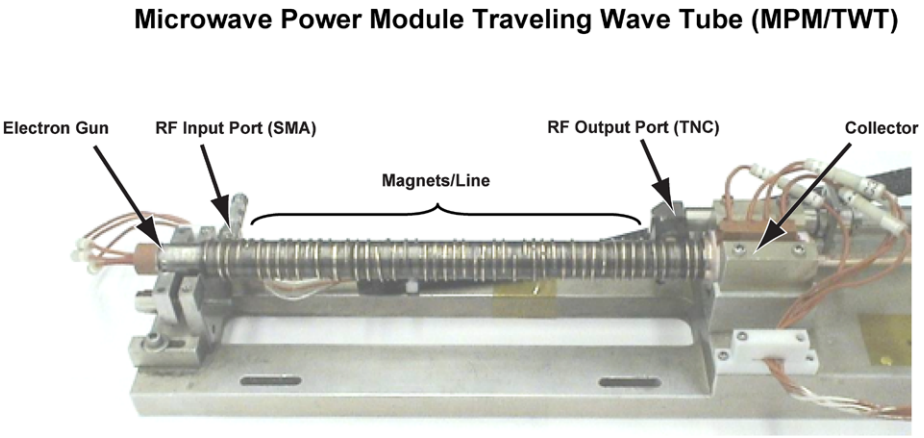

Fig. 9 Mini-RF Microwave Power Module Traveling Wave Tube (MPM/TWT)

it for spaceflight. The Mini-RF transmitter is based upon designs and processes developed over the last 15 years, with over 400 airborne units/year produced over the last two years. The primary Mini-RF transmitter challenge is adapting these proven airborne designs for space application. These include materials and part selection, outgassing, reliability, and radiation tolerance. The technical challenges overcome in the transmitter included developing low outgassing, high voltage insulators and space qualification parts screening for miniature high-voltage power supplies. The transmitter complied with the overall Mini-RF parts screening program which screened parts to a total dose of 20 kRad, no destructive latch-up, and tolerance of non-destructive latch up at 75 MeV. Meeting the stringent mass and power limitations required some parts to carry wavers but the overall parts' program was compatible with the Class S and LRO Class B requirement with de-rating criteria in accordance

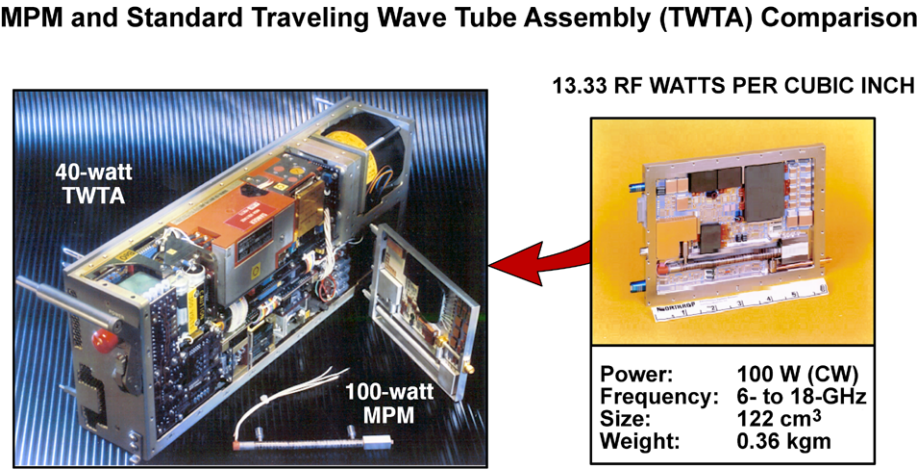

Fig. 10 Mini-RF transmitter module comparison

with established procedures. Mini-RF uses PEMs (Plastic Encapsulated Microcircuits) with the screening operable over the temperature range of −55 to +125°C. The MPM thermal design necessitated integration with the LRO heat-pipe system, which allowed for effective dissipation of heat generated by the transmitter.

Sandia National Laboratory (SNL) developed the Digital Receiver (DRX) and Quadrature Digital Wave Form Synthesizer (QDWS). These systems afford Mini-RF a degree of flexibility and reprogrammability not previously available in space-based systems. Over 1000 waveforms may be programmed. A processor module based on a heritage RAD 750 processor and associated firmware and software controls the Mini-RF system.

4.3 Interconnect Module

The Interconnect Module (IM) combines and splits the RF energy and serves as the interface between the transmitter, receiver, and antenna. Its design specifically handles issues such as multipaction using selected materials and geometry.

5 Calibration

Laboratory calibration data was acquired during spacecraft integration and test. The overarching goal of these activities was to insure production of a calibrated instrument. All waveforms in the waveform table were tested on brassboard hardware while selected waveforms were tested on flight hardware. This waveform testing is inherent in the overall Mini-RF integration and test program. Additional waveform testing was conducted on the flight instrument during thermal vacuum temperature ramp cycles. Internal calibration data are acquired every time that Mini-RF takes a data collect; a chirp, noise, and tone calibration is done both immediately before and immediately after a data collect. No end-to-end range tests were possible during integration and test, which necessitated the use of in-flight external calibration.

External calibration is planned in-flight by in conjunction with ground-based assets at the Greenbank and the Arecibo Radio Telescopes. These measurements will include polarization purity or axial ratio and antenna pattern. A transmitted signal from the LRO mini-RF is

received by Greenbank while the antenna pattern is scanned over a range of angles. Specifically, the scan will be $\pm 12^\circ$ from boresight in both elevation and azimuth, sampling at 0.5° increments. At each orientation, mini-RF will transmit for approximately 40 ms. Subsequently, each axis (azimuth or elevation) of the antenna will be parallel to the Earth's equator, with the boresight pointed towards Greenbank. The antenna will then be scanned parallel to the Earth's equator, at 0.4° per second 12° in one direction, then back to boresight, then 12° in the other direction, then back to boresight. During scanning, Mini-RF will transmit for 40 ms every 1.25 seconds, corresponding to an angle change between transmits of 0.5°. The scan should take approximately two minutes to complete. Next, the spacecraft will be rolled 90° so the other antenna plane is parallel to the Earth's equator, and the procedure will be repeated. The total time for the calibration should be approximately five minutes. An S-band received calibration will also be conducted using signals transmitted from Arecibo following the same geometry as the transmit calibration. An Arecibo X-band transmit calibration is under consideration. During commissioning, Mini-RF can acquire calibration data before the nominal science-mapping phase begins. At least two lunar equatorial areas will be imaged for calibration purposes most likely covering latitudes from 10° to -10° at 33° west longitude and 33° east longitude. Since each of these data acquisitions requires approximately six minutes and LRO Mini-RF may only transmit for four minutes, each equatorial target will be subdivided into two separate sequences. First, Mini-RF will image from 10°N to 2°S at 33° longitude on one orbit and then on the next orbit from 2°N to 10°S. These areas were chosen to have similar incidence angles as ground-based radar images collected over the same terrain to provide independent verification of Mini-RF measurements. The longitude of this second data take would be either 32° or 34°. Every six months there will be a window, centered around the dawn–dusk orbit, where calibration activities can be conducted, particularly calibration activities that require a spacecraft maneuver. During these times, Mini-RF can conduct the following calibration activities, in priority order; transmit calibration to Greenbank, two 1-minute nadir mode observations (ideally in a polar region), and a receive calibration from Arecibo using the same scan pattern used for the transmit calibrations. These calibration procedures have been tested successfully during the Chandrayaan-1 mission and experience gained will be applied to the LRO Mini-RF instrument. An example equatorial calibration image obtained by Chandrayaan-1's Forerunner Mini-SAR is shown in Fig. 11. An additional calibration is currently planned at X-band using the Goldstone Planetary Radar System. Radar data will be collected by Goldstone from the same lunar equatorial areas imaged by Mini-RF from lunar orbit at similar incidence angles.

6 Data Analysis, Interpretation, and Modeling

Following in-flight calibration, a set of coefficients will be derived and applied to the radar data as part of the standard processing stream (Fig. 12) prior to computing the Stokes parameters that in turn are used to calculate daughter products (e.g. CPR, degree of linear and circular polarization). A joint Chandrayaan/LRO Mini-RF Payload Operations Center (POC) is located at APL to support the Mini-RF experiments. The POC will provide the following functions: forward data acquisition sequences to GSFC, receive raw telemetry from GSFC, process raw telemetry, produce mosaics, and catalog data for the PDS and other repositories. The POC team is comprised of the POC lead engineers, Science Team representatives and the POC engineers. Figure 13 shows a high level view of the Mini-RF ground system and POC subsystems.

The POC will submit, to Goddard Space Flight Center (GSFC) for LRO, the command sequences that control the execution of the data acquisition and storage to the onboard flight

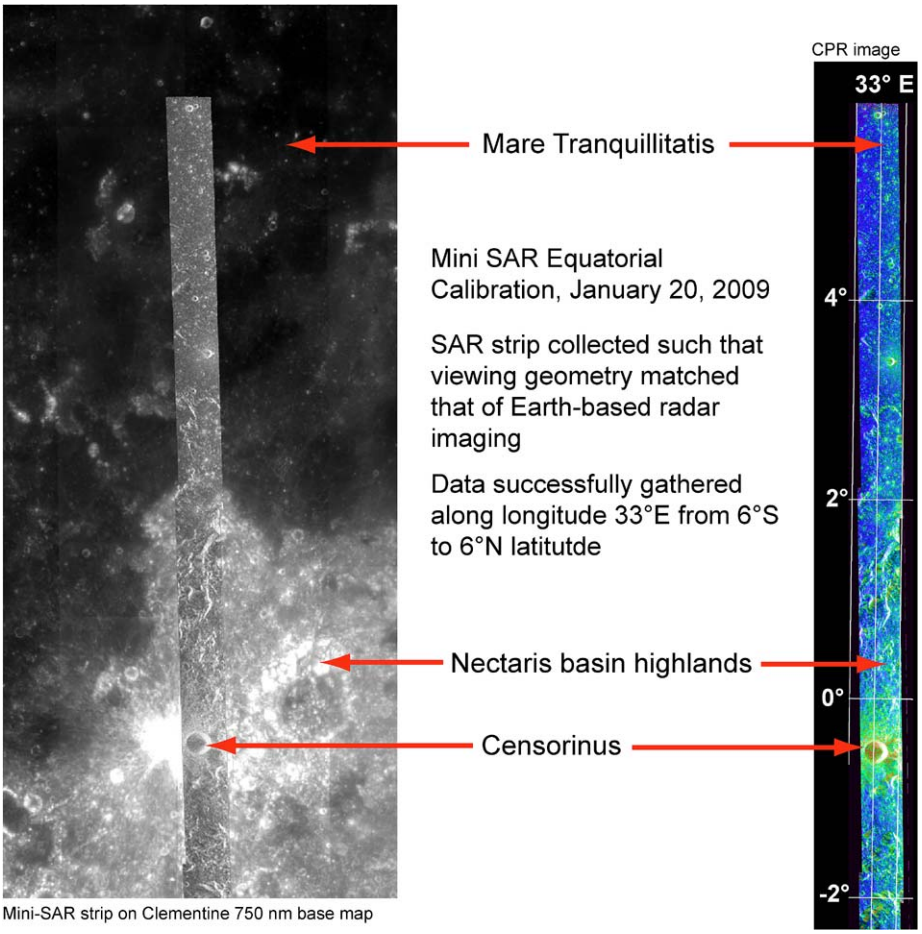

Fig. 11 Chandrayaan-1 flight calibration image

recorder. The Calibration and Collect commands have embedded argument lists that configure the radar with respect to waveform, pulse repetition frequency (PRF), pulse width, burst time, burst duty factor, number of bursts, position of receiving gate, bandwidth, start frequency, and other supporting parameters.

Once the acquired data and the required ancillary data have been received by the POC, the data will be processed according to the data type. This processing will use the ephemeris data supplied to the POC to create products to be checked for completeness and quality. All processed science products, science and housekeeping telemetry, ancillary products and command files are archived within the POC. Science products are also delivered to the Planetary Data System (PDS) for public release. The data processing architecture and calibration procedures to be used for LRO have been tested and validated using data from Forerunner Mini-SAR on Chandrayaan-1.

Acknowledgements We would like to acknowledge Susan Selkirk of Arizona State University School of Earth and Space Exploration for her support of graphics and related efforts in preparation of this paper. This paper is an LPI contribution #.

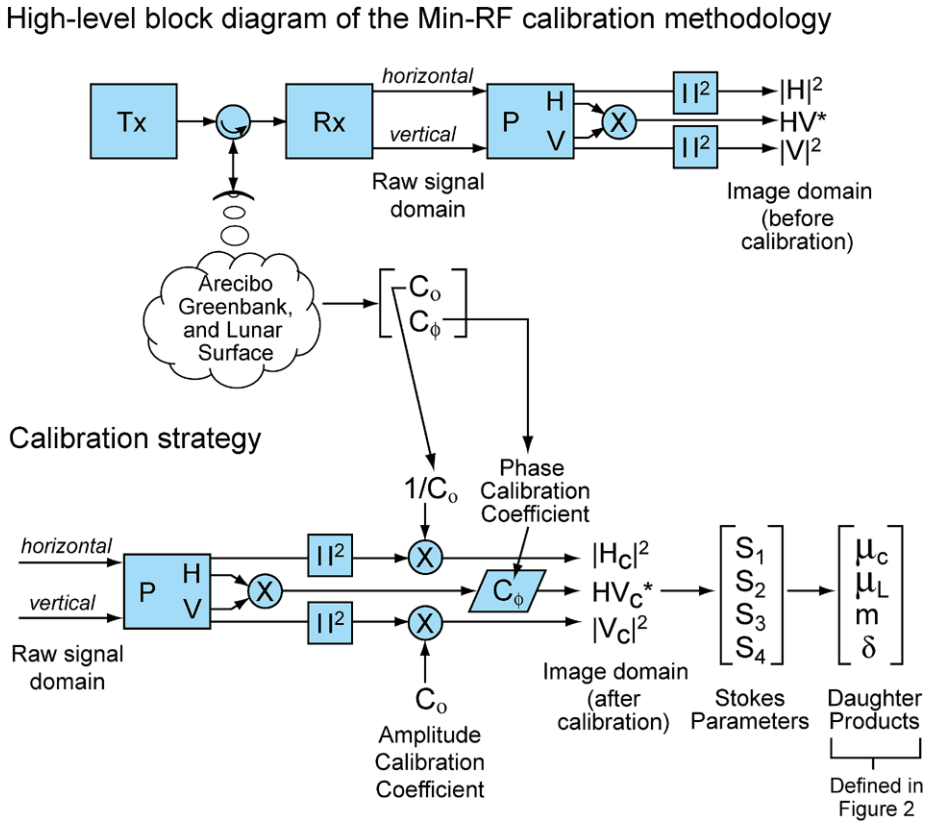

Fig. 12 Mini-RF calibration strategy

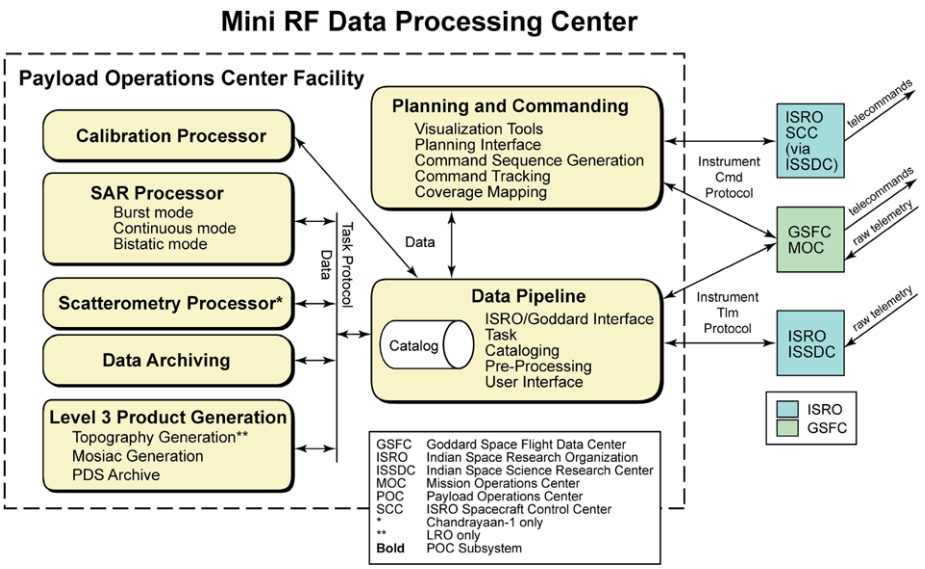

Fig. 13 POC overview

References

J.R. Arnold, Ice in the lunar polar regions. J. Geophys. Res. **84**, 5659–5668 (1979)
B. Butler, The migration of volatiles on the surfaces of Mercury and the Moon. J. Geophys. Res. **102**, 19,283–19,291 (1997)
D.B. Campbell, B.A. Campbell, L.M. Carter, J.-L. Margot, N.J.S. Stacy, No evidence for thick deposits of ice at the lunar South Pole. Nature **443**, 835–837 (2006)
R.C. Elphic, V.R. Eke, L. Teodoro, D.J. Lawrence, D.B.J. Bussey, Models of the distribution and abundance of hydrogen at the lunar South Pole. Geophys. Res. Lett. **34**, L13204 (2007). doi:10.1029/2007GL029954
W.C. Feldman, S. Maurice, A.B. Binder, B.L. Barraclough, R.C. Elphic, D.J. Lawrence, Fluxes of fast and epithermal neutrons from lunar prospector: evidence for water ice at the lunar poles. Science **281**, 1496–1500 (1998)
W.C. Feldman, D.J. Lawrence, R.C. Elphic, B.L. Barraclough, S. Maurice, I. Genetay, A.B. Binder, Polar hydrogen deposits on the Moon. J. Geophys. Res. **105**(E2), 4175–4195 (2000)
J.K. Harmon, M.A. Slade, Radar mapping of Mercury: Full-disk Doppler delay images. Science **258**, 640–643 (1992)
M.I. Mishchenko, Polarization characteristics of the coherent backscatter opposition effect. Earth Moon Planets **58**, 127–144 (1992)
H. Noda, H. Araki, S. Goossens, Y. Isihara, K. Matsumoto, S. Tazawa, S. Sasaki, N. Kawano, S. Sasaki, Illumination conditions at the lunar polar regions by Kaguya (SELENE) laser altimeter. Geophys. Res. Lett. **35**, L24203 (2008). doi:10.1029/2008GL035692
S. Nozette, C. Lichtenberg, P.D. Spudis, R. Bonner, W. Ort, E. Malaret, M. Robinson, E.M. Shoemaker, The Clementine bistatic radar experiment. Science **274**, 1495–1498 (1996)
S. Nozette, E.M. Shoemaker, P.D. Spudis, C.L. Lichtenberg, The possibility of ice on the Moon. Science **278**, 144–145 (1997)
S. Nozette, P.D. Spudis, M. Robinson, D.B.J. Bussey, C. Lichtenberg, R. Bonner, Integration of lunar polar remote-sensing data sets: Evidence for ice at the lunar South Pole. J. Geophys. Res. **106**(E19), 23253–23266 (2001)
R.K. Raney, Hybrid-polarity SAR architecture. IEEE Trans. Geosci. Remote Sens. **45**, 3397–3404 (2007)
R.A. Simpson, G.L. Tyler, Reanalysis of Clementine bistatic radar data for the lunar South Pole. J. Geophys. Res. **104**, 3845–3862 (1999)
P.D. Spudis, Ice on the Moon. Space Rev. (2006). http://www.thespacereview.com/article/740/1
P. Spudis, S. Nozette, B. Bussey, K. Raney, H. Winters, C.L. Lichtenberg, W.M. Marinelli, J.C. Crusan, M.M. Gates, Mini-SAR: An imaging radar experiment for the Chandrayaan-1 mission to the Moon. Curr. Sci. (India) **96**, 533–539 (2009)
N.J.S. Stacy, High-resolution synthetic aperture radar observations of the moon. Ph.D. dissertation, Cornell University, Ithaca, NY (1993)
N.J.S. Stacy, D.B. Campbell, P.G. Ford, Arecibo radar mapping of the lunar poles: A search for ice deposits. Science **276**, 1527–1530 (1997)